

# Optimized Electrochemical Detection of Anti-Cancer Drug by Carbon Nanotubes or Gold Nanoparticles

Nima Aliakbarinodehi\*, Giovanni De Micheli, Sandro Carrara  
Integrated Systems Laboratory, École Polytechnique Fédérale de Lausanne (EPFL)  
Lausanne, Switzerland

\* nima.aliakbarinodehi@epfl.ch

**Abstract**—Nanostructured biosensors with the aim of electroactive cancer-drug detection were investigated. The aim of this work is improvement of the sensitivity and limit of detection of two differently nanostructured biosensors to find out the best choice for quantifying the concentration of etoposide, as a widely used electroactive cancer drug, in its therapeutic range. To this purpose etoposide concentrations, ranging from zero to 60  $\mu\text{M}$ , were sensed at multi-walled carbon nanotube and gold nanoparticle functionalized bioelectrodes using cyclic voltammetry. The optimum scan rate for voltammetric experiments was found out equal to 70  $\text{mV s}^{-1}$  and 130  $\text{mV s}^{-1}$  for multi-walled carbon nanotube and gold nanoparticle based electrodes, respectively. For nanostructuring the electrodes, the optimum nanomaterial mass were experimentally obtained for multi-walled carbon nanotube and gold nanoparticle based electrodes equal to 20  $\mu\text{g}$  (4314  $\text{mm}^2$  of additional electroactive surface area) and 104  $\mu\text{g}$  (6471  $\text{mm}^2$  of additional electroactive surface area), respectively. Bioelectrodes produced based on this optimized configurations showed sensitivity of  $0.98 \pm 0.41 \mu\text{A } \mu\text{M}^{-1} \text{cm}^{-2}$  and  $1.43 \pm 0.26 \mu\text{A } \mu\text{M}^{-1} \text{cm}^{-2}$ , and limit of detection of  $1.52 \pm 0.89 \mu\text{M}$  and  $1.29 \pm 0.48 \mu\text{M}$  for multi-walled carbon nanotube and gold nanoparticles based electrodes. Comparing the limit of detection achieved in this work with the therapeutic range of etoposide verifies the possibility of using both nanostructured bioelectrodes for etoposide detection. However, gold nanoparticle based electrodes exhibit better electrochemical improvements in terms of both sensitivity and limit of detection.

**Keywords**—nanostructure properties, electrochemical detection, gold nanoparticle, carbon nanotube, cyclic voltammetry, electroactive cancer-drug detection

## I. INTRODUCTION

Electrochemical metabolite detection using nanostructured bioelectrodes as sensing element are very attractive for point of care therapeutic drug monitoring (TDM), or in other words the individualization of the dosing regime to maintain the blood drug concentration within a beneficiary range that is called therapeutic range. This is more significant for cancer drugs, which are mainly toxics, and have normally very narrow therapeutic ranges; prescribing a dosing regime for them, as a result, for a wide range of patients with different genetic profile and cultural background is very difficult. Others have investigated the effectiveness of the TDM in terms of the additional costs (time and money) of the process in reducing

the mortality and morbidity of the diseases [1]. This shows the need for a low cost and fast TDM process, which also ensures the good enough communication between the TDM team members for better interpretation of the results [2][3][4]. Electrochemical bioelectrodes have shown to be a promising system to replicate the time-consuming and costly laboratory experiments and analysis that are used for TDM, currently. Therefore, they can be the connection between TDM and site testing, emergency room screening, bedside monitoring and home self-testing [5][6]. Electrochemical bioelectrodes provide an interface between redox site of target metabolite and electronic part of the biosensors. Most bioelectrodes act as transducers to convert biological events to electric current by applying a fixed potential over the electrode and target (amperometry), or sweeping the applied potential in a range (voltammetry) and measuring the current. Amperometry experiments are beneficial because of their high sensitivity and large linear range, whilst voltammetry experiments provide the option of multi-target detection [7]. Many different enzymatic [3][9][10] and non-enzymatic [10][11][12] bioelectrodes have been proposed in literature that can be useful to this purpose. The role of nanostructuring in enhancing the electrochemical performance of bioelectrodes is widely studied and reported [13][14][15], but at our best knowledge there are not enough work done on the impact of physical nature of the different nanomaterials on the performance. The different effect of multi-walled carbon nanotubes (MWCNTs) and gold nanoparticles (GNPs) on enhancing the sensitivity and limit of detection (LOD) of  $\text{H}_2\text{O}_2$ -bioelectrodes is investigated somewhere else [16]. Similarly, direct electron transfer by enzymes has been investigated on MWCNT [17] and GNPs [9]. Moreover, nanoparticles are well know to support quantum phenomena both in case of conductive [18] and semiconductives ones [19]. The aim of this work is to compare and investigate the natural properties of the MWCNTs and GNPs on improving the performance of bioelectrodes for electroactive-drug detection. The optimum performance by means of each nanomaterial is obtained by modifying the additional ElectroActive Surface Areas (EASA) and scan rate of voltammetry experiments. Then the sensitivity of produced bioelectrodes with these optimized configurations are compared to figure out which one can be the better choice for biosensing applications.

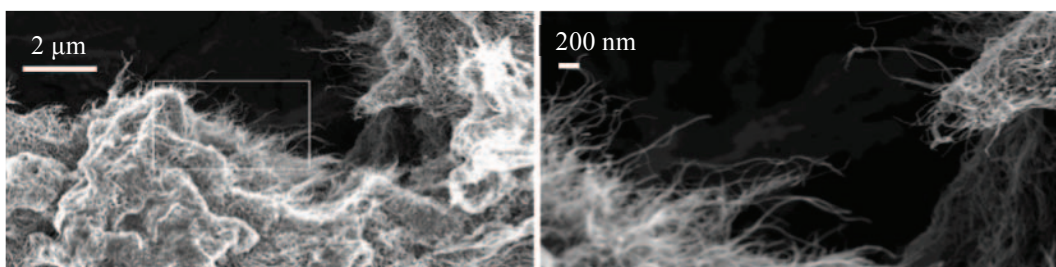


Figure 1, SEM images of MWCNTs that were taken after deposition over the working electrode of a SPE. Left figure shows surface of working electrode, which is covered by MWCNTs. Right figure, is the magnification of the specified area on the left figure. MWCNTs have average diameter of 10 nm and length of 1 - 2  $\mu\text{m}$ .

## II. MATERIAL AND METHODS

### A. Nano materials

Biosensors were fabricated based on commercial screen-printed electrodes (SPEs) manufactured by Metrohm (DRP-110). They consist of graphite working electrode (area – 0.12  $\text{cm}^2$ ), graphite counter electrode and silver reference electrode. Powder of MWCNTs (diameter: 10 nm; length: 1 to 2  $\mu\text{m}$ ; 90% purity), functionalized with COOH was purchased from DropSens (Spain), which was dispersed in chloroform to the concentration of 1  $\text{mg mL}^{-1}$ , and was sonicated for 1 hour to achieve a homogenous solution. Dispersion of hydrophilic Gold nanoparticles (GNPs; OD-1; 0.06  $\text{mg mL}^{-1}$ ), functionalized with Tannic acid, with average diameter of  $5.22 \pm 0.01$  nm (Fig. 2) was purchased from Sigma-Aldrich. Phosphate buffer saline (PBS-100mM; pH-7.4) was provided by Sigma-Aldrich, and solved in distilled water and stirred to obtain the homogenous solution. It was used as supporting electrolyte in experiments. Etoposide powder was purchased from Sigma-Aldrich and was dissolved in dimethyl sulfoxide (DMSO) to the concentration of 10 mM.

### B. Electrode preparation

Functionalization of SPEs with nanostructures was carried out exploiting drop-casting technique for ease of action and minimizing the interferences. For instance, to prepare SPEs equipped with hydrophilic GNPs (GNP-SPEs), 290  $\mu\text{l}$  of 0.06  $\text{mg mL}^{-1}$  stock dispersion was dropped over the working electrode (W.E.) in steps of 10  $\mu\text{l}$  to obtain overall mass of 17.4  $\mu\text{g}$  of GNPs. Electrodes were stored at ambient temperature after each deposition for drying, and also for storage. Electroactive surface areas (EASA) have been calculated using specific surface area of each material and amount of deposited mass used for electrode preparation [20]. EASA has been used

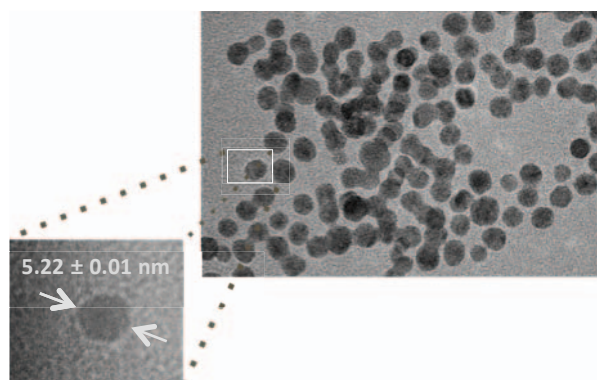


Figure 2, TEM image of hydrophilic sample of GNPs with average diameter of  $5.22 \pm 0.01$  nm. One spherical GNP is pointed out on the left figure.

as the unit rather than mass to provide reasonable comparison between electrodes equipped with different types of nanomaterials, following the previous work of this group [16]. For scan rate optimization 3 electrodes were equipped with the optimized amount of MWCNTs (30  $\mu\text{g}$  – 6471  $\text{mm}^2$  of EASA) and GNPs (69.6  $\mu\text{g}$  - 4314  $\text{mm}^2$  of EASA). To optimize the amount of nanomaterial used for deposition (deposition mass optimization), 3 sets of electrodes were produced. Each set contained 9 electrodes equipped with MWCNTs ranging from 0 to 40  $\mu\text{g}$  with step of 5  $\mu\text{g}$  (bare SPE, MWCNT-SPE-1078, MWCNT-SPE-2157, ..., MWCNT-SPE-8628). Next, same process were done to prepare 3 sets of GNP-SPEs (bare SPE, GNP-SPE-1078, ..., GNP-SPE-8628). For instance, 17.4  $\mu\text{g}$  of GNPs were deposited over W.E. of an electrode to produce GNP-SPE-1078. TEM (Fig. 2) and SEM images (Fig. 1) have been taken using Tecnai Osiris device, and MERLIN device, respectively. All image analyses have been performed utilizing ImageJ software [21].

### C. Electrochemical measurement apparatus and setup

Autolab potentiostat/galvanostat (PGSTAT128N) was used for cyclic voltammetry (CV) under aerobic conditions. To obtain the Voltammograms, first 100  $\mu\text{l}$  of etoposide solution (PBS; pH-7.4; as background electrolyte) covered the active part of the electrode. Device was configured to swap the voltage between -1 and +1 for 10 cycles to achieve a stable result.

## III. ELECTROCHEMICAL EXPERIMENTS AND RESULTS

Electrochemical experiments started with two optimization steps: first, to figure out the best protocol for electrode preparation in terms of the amount of mass for deposition. Second, to find out the optimum scan rate used in voltammetry experiments in order to get highest peak amplitude.

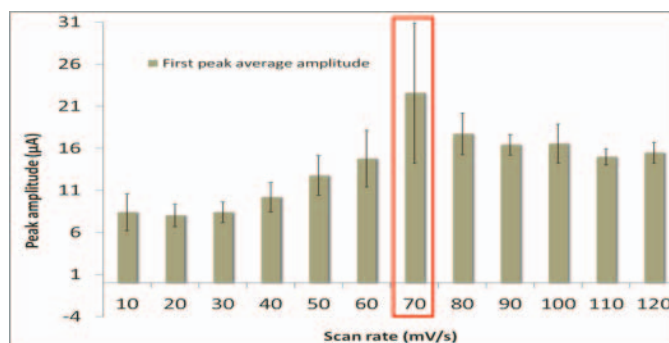


Figure 3, Averaged oxidation peak amplitude of etoposide. Electrodes were equipped with 6471  $\text{mm}^2$  of EASA using 30  $\mu\text{g}$  of MWCNTs and examined in a range of scan rate from 10 to 120  $\text{mVs}^{-1}$

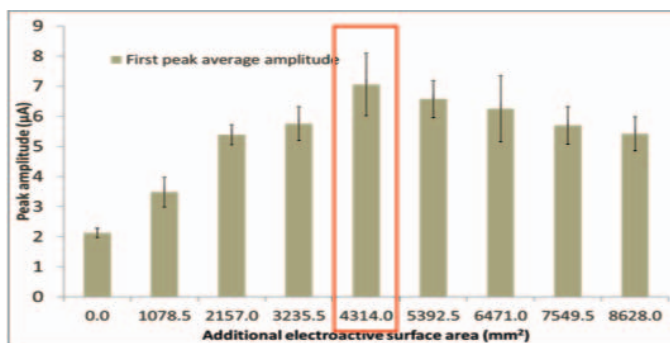


Figure 4, Averaged oxidation peak amplitude related to etoposide detection using CV technique. Scan rate were fixed to  $70 \text{ mV s}^{-1}$  and SPEs were nanostructured with different amount of EASA as shown on the horizontal axis of the graph.  $4314 \text{ mm}^2$  demonstrates highest peak amplitude.

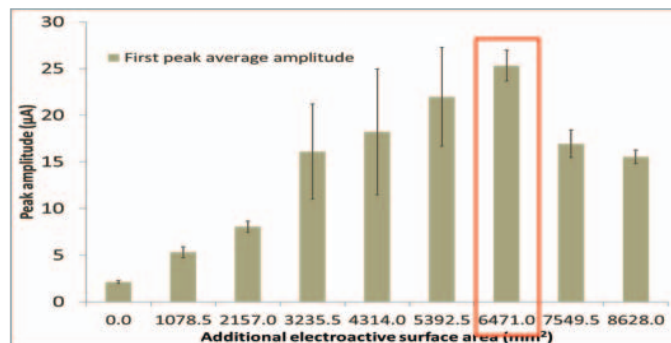


Figure 6, Averaged oxidation peak amplitude related to etoposide detection using CV technique. Scan rate were fixed to  $130 \text{ mV s}^{-1}$  and SPEs were nanostructured with different amount of EASA as shown on the horizontal axis of the graph.  $6471 \text{ mm}^2$  demonstrates highest peak amplitude.

### A. MWCNT-SPEs optimization

To find out the best scan rate for CV the deposition mass was fixed to  $6471 \text{ mm}^2$  ( $30 \mu\text{g}$  of MWCNTs). Concentration of etoposide in the target solution was set to  $70 \mu\text{M}$  at this step (Etop-70). Three electrodes were prepared with this configuration and were tested using CV while varying the scan rate in a range of  $10 \text{ mV s}^{-1}$  to  $120 \text{ mV s}^{-1}$ , with step of  $10 \text{ mV s}^{-1}$ .

Acquired voltammograms (data not shown) have been analyzed by Nova software to obtain the measured peak amplitudes (Fig. 3). Based on these data, scan rate of  $70 \text{ mV s}^{-1}$  can provide highest peak amplitude for MWCNT-SPEs. This scan rate has been used for next optimization step and sensitivity experiments of MWCNT-SPEs. At second optimization step, MWCNT-SPEs were prepared with EASA ranging from zero (bare-SPE) to  $8628 \text{ mm}^2$  as explained earlier, and practiced by CV to detect Etop-70. Scan rate of CV experiment was fixed to the result of the last step ( $70 \text{ mV s}^{-1}$ ). After analyzing the results the average of peak amplitudes are presented in Fig. 4. SPEs equipped with  $4314 \text{ mm}^2$  of additional EASA have exhibited highest peak amplitude. As a result, this deposition configuration and  $70 \text{ mV s}^{-1}$  as scan rate was used for MWCNTs-SPEs sensitivity experiments.

### B. GNP-SPEs optimization

Scan rate and deposition mass optimization for GNP-SPEs were carried out with the same process as described for MWCNT-SPEs. The only differences were the deposited EASA ( $4314 \text{ mm}^2$ ) and the maximum tested scan rate ( $150 \text{ mV s}^{-1}$ ) for scan rate optimization of GNP-SPEs. Acquired

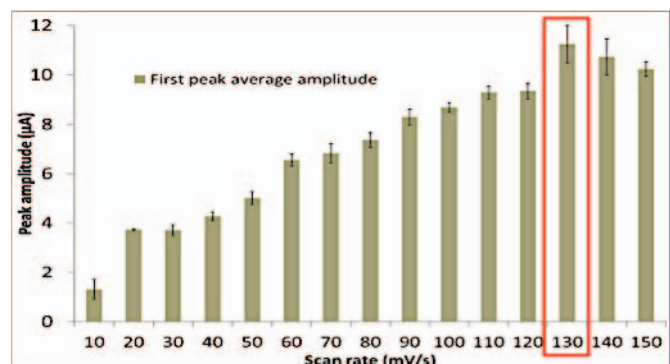


Figure 5, Averaged oxidation peak amplitude of etoposide. Electrodes were equipped with  $4314 \text{ mm}^2$  of EASA using  $69.6 \mu\text{g}$  of GNPs and examined in a range of scan rate from 10 to  $150 \text{ mV s}^{-1}$ .

averaged peak amplitudes for scan rate and EASA optimizations are presented in Fig. 5 and Fig. 6 respectively. The scan rate extension to  $150 \text{ mV s}^{-1}$  was due to the fact that the peak was growing until  $130 \text{ mV s}^{-1}$ .

According to the data presented by the graph,  $130 \text{ mV s}^{-1}$  and  $6471 \text{ mm}^2$  were chosen for GNP-SPE as experiment and electrode preparation configurations.

### C. Sensitivity and limit of detection comparison

To compare the MWCNT-SPEs and GNP-SPEs in terms of sensitivity and LOD, three electrodes were produced for each nanomaterial using optimum additional EASA and tested by CV using optimum scan rate configuration. Concentration of target solution, etoposide (PBS as background solution), was increased from 0 (blank measurement) to  $60 \mu\text{M}$  in steps of  $10 \mu\text{M}$ , corresponding to the therapeutic range of etoposide [22]. Acquired voltammograms related to the experiments performed on MWCNT-SPEs and hydrophilic GNP-SPEs are not shown here. Peak amplitudes were analyzed and measured for different concentrations of etoposide to obtain calibration curve. LODs were calculated using the standard deviation of three blank measurements related to each set of MWCNT-SPEs and GNP-SPEs [23]. Calibration curves and measured data related to sensitivity and LODs are presented in Fig. 7 and Table 1 respectively. Presented data shows better performance for GNP-SPEs in terms of either sensitivity or LOD.

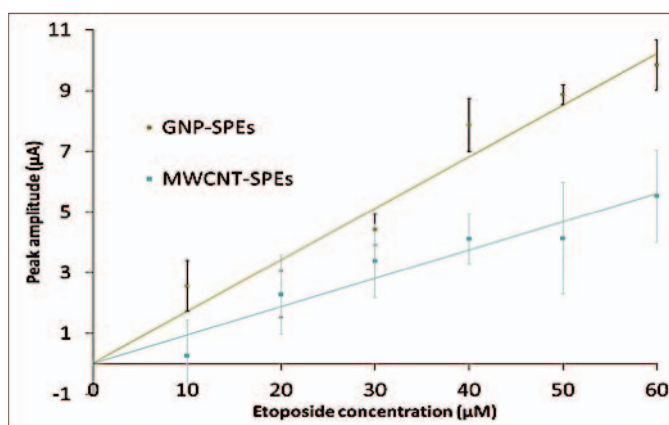


Figure 7, Calibration curves related to GNP-SPEs and MWCNT-SPEs are presented in this figure for comparison. These electrodes were prepared using  $6471$  and  $4314 \text{ mm}^2$  of additional EASA respectively, and were experimented with CV to detect etoposide with concentration varying from 0 to  $60 \mu\text{M}$  as is shown on the horizontal axis. Scan rates were set to  $130$  and  $70 \text{ mV s}^{-1}$ , respectively. Data points are shifted, to provide more clarity of sensitivity differences, by  $2.95 \mu\text{A}$  and  $1.2 \mu\text{A}$  for MWCNT-SPEs and GNP-SPEs respectively.

TABLE I. ELECTROCHEMICAL RESULTS RELATED TO MWCNT-SPEs AND HYDROPHILIC GNP-SPEs ARE PRESENTED FOR COMPARISON

	<i>Sensitivity (<math>\mu\text{A}\mu\text{M}^{-1}\text{cm}^{-2}</math>)</i>	<i>LOD (<math>\mu\text{M}</math>)</i>
MWCNT-SPEs	$0.98 \pm 0.41$	$1.52 \pm 0.89$
GNP-SPEs	$1.43 \pm 0.26$	$1.29 \pm 0.48$

#### IV. CONCLUSION

Better electrochemical properties of GNP-SPEs (5 nm in diameter) respect to MWCNT-SPEs (higher sensitivity and better LOD) on detection of etoposide are experimentally proven. This enhancement is partly owing to higher affinity of hydrophilic GNPs to electroactive xenobiotics as etoposide, and partly due to the small dimension of nanoparticles. Taking into account that both functionalized electrodes were tested at their optimum configurations, it can be inferred that the size of nanoparticles that is under the 10 nm have taken a significant role. This is already discussed that GNPs with decreasing diameter can provide electrochemical enhancements. For instance, in [24] it is presented that by decreasing the size of GNPs from 13 nm to 6 nm and then to 3.5 nm, maximum current is increased to 66.2  $\mu\text{A}$ , 73.8  $\mu\text{A}$ , and 76.2  $\mu\text{A}$ , respectively. However, this phenomenon is not observed experimentally on electroactive drug detection. Low enough LOD, high sensitivity (even at very low concentrations) and simple functionalization make the proposed GNP-SPEs a suitable option for detection of electroactive drugs as etoposide. Nevertheless, there are some other factors to be addressed including the effect of nanoparticles dimension on the performance and the physics behind it, which is the target of this group future works.

#### V. ACKNOWLEDGEMENT

This research was supported partly by the project PROSENSE funded by the European Union's Horizon 2020 research and innovation programme under the grant agreement no 317420, and partly by ERC-2009-AdG-246810.

#### REFERENCES

[1] Touw, D. J., et al. "Cost-effectiveness of therapeutic drug monitoring: a systematic review." *Therapeutic drug monitoring* 27.1 (2005): 10-17. J. Clerk Maxwell, A Treatise on Electricity and Magnetism, 3rd ed., vol. 2. Oxford: Clarendon, 1892, pp.68-73.

[2] Gross, Annette S. "Best practice in therapeutic drug monitoring." *British journal of clinical pharmacology* 46.2 (1998): 95-99.

[3] Carrara, Sandro, et al. "Multi-panel drugs detection in human serum for personalized therapy." *Biosensors and Bioelectronics* 26.9 (2011): 3914-3919.R.

[4] C Baj-Rossi, GD Micheli, S Carrara, Electrochemical detection of anti-breast-cancer agents in human serum by cytochrome P450-coated carbon nanotubes, *Sensors* 12 (2012), 6520-6537.

[5] Wang, Joseph. "Amperometric biosensors for clinical and therapeutic drug monitoring: a review." *Journal of pharmaceutical and biomedical analysis* 19.1 (1999): 47-53.

[6] Wang, Joseph. "Electrochemical biosensors: towards point-of-care cancer diagnostics." *Biosensors and Bioelectronics* 21.10 (2006): 1887-1892.

[7] Baj-Rossi, Camilla, et al. "Full Fabrication and Packaging of an Implantable Multi-Panel Device for Monitoring of Metabolites in Small Animals." (2014).

[8] Joseph, Shiba, et al. "An amperometric biosensor with human CYP3A4 as a novel drug screening tool." *Biochemical pharmacology* 65.11 (2003): 1817-1826.

[9] Shumyantseva, Victoria V., et al. "Direct electron transfer between cytochrome P450scc and gold nanoparticles on screen-printed rhodium-graphite electrodes." *Biosensors and Bioelectronics* 21.1 (2005): 217-222.

[10] Baj-Rossi, Camilla, Giovanni De Micheli, and Sandro Carrara. "Electrochemical detection of anti-breast-cancer agents in human serum by cytochrome P450-coated carbon nanotubes." *Sensors* 12.5 (2012): 6520-6537.

[11] Xiao, Fei, et al. "Sensitive voltammetric determination of chloramphenicol by using single-wall carbon nanotube-gold nanoparticle-ionic liquid composite film modified glassy carbon electrodes." *Analytica chimica acta* 596.1 (2007): 79-85.

[12] Ploegmakers, H. H. J. L., et al. "Computerized cyclic voltammetric detection after HPLC of the antineoplastic agents etoposide, teniposide, adriamycin and its metabolite adriamycinol in urine samples." *Journal of Analytical Methods in Chemistry* 11.3 (1989): 106-112.

[13] Bharathi, Subramanian. "Sol-gel-derived nanocrystalline gold-silicate composite biosensor." *Anal. Commun.* 35.1 (1998): 29-31.

[14] Authier, Laurent, et al. "Gold nanoparticle-based quantitative electrochemical detection of amplified human cytomegalovirus DNA using disposable microband electrodes." *Analytical chemistry* 73.18 (2001): 4450-4456.

[15] Tang, Hao, et al. "Amperometric glucose biosensor based on adsorption of glucose oxidase at platinum nanoparticle-modified carbon nanotube electrode." *Analytical Biochemistry* 331.1 (2004): 89-97.

[16] Aliakbarinodehi, N., Taurino, I., Pravin, J., Tagliaferro, A., Piccinini, G., De Micheli, G., & Carrara, S. (2015). Electrochemical nanostructured biosensors: carbon nanotubes versus conductive and semi-conductive nanoparticles. *Chemical Papers*, 69(1), 134-142.

[17] S Carrara, VV Shumyantseva, AI Archakov, B Samori, Screen-printed electrodes based on carbon nanotubes and cytochrome P450scc for highly sensitive cholesterol biosensors, *Biosensors and Bioelectronics* 24 (2008), 148-150

[18] Daniel, Marie-Christine, and Didier Astruc. Gold nanoparticles: assembly, supramolecular chemistry, quantum-size-related properties, and applications toward biology, catalysis, and nanotechnology, *Chemical reviews* 104.1 (2004): 293-346.

[19] V Erokhin, S Carrara, H Amenitch, S Bernstorff, C Nicolini, Semiconductor nanoparticles for quantum devices, *Nanotechnology* 9 (1998), 158

[20] Peigney, A., Laurent, C., Flahaut, E., Bacsu, R. R., & Rousset, A. (2001). Specific surface area of carbon nanotubes and bundles of carbon nanotubes. *Carbon*, 39(4), 507-514.

[21] Schneider, C. A., Rasband, W. S., Eliceiri, K. W., Schindelin, J., Arganda-Carreras, I., Frise, E., ... & Roesam, B. (2012). 671 nih image to imageJ: 25 years of image analysis. *Nature methods*, 9(7).

[22] Arbuick, Susan G., et al. "Etoposide pharmacokinetics in patients with normal and abnormal organ function." *Journal of Clinical Oncology* 4.11 (1986): 1690-1695.

[23] Mocak, J., Bond, A. M., Mitchell, S., & Scollary, G. (1997). A statistical overview of standard (IUPAC and ACS) and new procedures for determining the limits of detection and quantification: application to voltammetric and stripping techniques. *Pure and Applied Chemistry*, 69(2), 297-328.

[24] German, Natalija, et al. "Glucose biosensor based on glucose oxidase and gold nanoparticles of different sizes covered by polypyrrole layer." *Colloids and Surfaces A: Physicochemical and Engineering Aspects* 413 (2012): 224-2